CHALMERS

Modeling and Simulation of a Cooling System for Ground Radar

Master of Science Thesis

LINUS JOHANSSON

Department of Signals and Systems
CHALMERS UNIVERSITY OF TECHNOLOGY
Göteborg. Sweden, 2012
Report No. EX008/2012

REPORT NO. EX008/2012

Modeling and Simulation of a Cooling System for Ground Radar

LINUS JOHANSSON

Department of Signals and Systems
CHALMERS UNIVERSITY OF TECHNOLOGY
Göteborg. Sweden 2012

Modeling and Simulation of a Cooling System for Ground Radar
Linus Johansson

Technical Report No. EX008/2012
Department of Signals and Systems
Chalmers University of Technology
SE-412 96 Göteborg
Sweden
Telephone +46 (0)31-772 1000

Chalmers Reproservice
Göteborg, Sweden 2012

Modeling and Simulation of a Cooling System for Ground Radar
LINUS JOHANSSON
Department of Signals and Systems
Chalmers University of Technology

Abstract

In this project, the cooling system for SAAB EDS's ground radar (ARTHUR) has been modeled and simulated. ARTHUR needs to be updated and a model of the cooling system could be helpful when making improvements to the system. The cooling system is water and glycol based and it essentially cools four different subsystems, including electronics, operator room and a radar system. The control of the cooling system is achieved by proportionally adjusting the water flow into each subsystem using analogue mechanical control valves (AVTA), which are subject to investigation in this project. Experiments have been performed on the AVTA valves where the control range and dynamic behavior of the valves have been determined. Further, the cooling system has been characterized and modeled for operation in hot ambient temperature (55 ˚C). The model has been implemented in Simulink and the simulation results have been compared with temperature data available from a previous test on the ground radar. From the comparison, one can conclude that the model provides an indication of the time it takes to reach different set point temperatures in the system. Moreover, simulation results give an overview of the cooling system and clarify the effects that the valve configurations have to the system. In connection to the evaluation of the present control new alternatives for control have been considered. A possible replacement of the AVTA valves is a PLC together with several new sensors and electrically controlled valves, which could increase flexibility by enabling modification of the set point temperatures during operation.

Acknowledgement

I would like to thank all SAAB EDS employees who have been involved in this project and by some means have contributed to the results presented in this report. Above all I would like to thank my supervisor Peter Bung for his guidance, support and patience throughout this project. Thanks are also directed to Hans Falk for the great discussions we have had; I am very grateful that you have shared your knowledge with me. Further, I would like to thank Jan Rydén and Torgny Hansson for having faith in me and accepting me for this project as well as planning and administrating this project. I would also like to thank all of you at SAAB EDS who attended my thesis presentation at the office in Kallebäck, December 2011.

Furthermore, I would like to thank Torsten Wik, the supervisor and examiner at Chalmers, who have contributed with important comments and guidance during the time frame of this project.

Last but not least, I would like to thank my family, my friends and my girlfriend for all their support during the work with this thesis. It would not have been possible without you.

Linus Johansson

Göteborg

January 2012

Contents

Nomenclature

Abbreviations

ACU	Air Conditioning Unit
ARTHUR	Artillery Hunting Radar
EGW	Ethylene Glycol Water
LCU	Liquid Cooling Unit
PAO	Polyalphaolefin
SDU	Signal Data Unit
TRU	Transmitter Unit
TWT	Travelling Wave Tube
TWT-CU	Travelling Wave Tube – Cooling Unit

Symbols

A	Area [m^2]
C_p	Specific heat capacity [kJ / (kg · K)]
K_v	Valve opening coefficient [(dm^3/s) / bar]
k	Heat transfer coefficient [Watt / (A · K)]
k_i	Heat transfer coefficient, where *i* defines which subsystem the coefficient refers to [Watt / K]
$k_{hx,i}$	Heat transfer coefficient for heat exchanger, where *i* defines which heat exchanger that is referred to [Watt / K]
m_i	Mass, where *i* defines which subsystem [kg]
$\dot{m}$	Mass flow [kg/s]
p	Pressure [bar]
Q	Power [Watt]
$Q_{ACU_{int}}$	Internal energy of the cabin's mass and the air inside of it [Watt]
$Q_{i_{ss}}$	Power at steady state, where *i* defines which subsystem the power refers to [Watt]
Q_{op}	Heating power from operators [Watt]
q	Volume flow [dm^3/s]
$T_{c,i}$	Temperature of cooling EGW, where *i* refer to a location of EGW [K]
T_i	Temperature, where *i* defines which temperature it refers to [K]
t	Time [s]
τ_i	Time constant, where *i* defines which constant it refers to [s or min]

List of Figures

List of Tables

1 Introduction

This report will present the project that has served as the author's Master of Science thesis, which has been performed at Chalmers University of Technology. The project has been carried out in collaboration with SAAB Electronic Defence Systems, located in Kallebäck, Göteborg.

1.1 Background

SAAB EDS develop and manufacture military radar systems for many applications, including air surveillance and artillery localization. For these systems there is a need for climate control of electronics, radar equipment and the operator's environment. The radar system, with product name ARTHUR, that will be the main focus of this thesis uses a water and glycol based cooling system. SAAB EDS has other products with similar cooling systems and some results of this thesis might apply to them as well. However, reference to the cooling system in this report will refer to ARTHUR's cooling system.

The present cooling system does the job fairly well but there are a few things that SAAB EDS would like to improve in order to have more confidence in the cooling system. The control is a setup with analogue valves that proportionally change the flow of cooling water into four different subsystems. A change of temperature for a bulb sensor will result in a movement of a valve's cone and consequently close or open the valve. The valves are in some sense self-regulating but they are unfortunately not very intelligent and their performance and characteristics have not been investigated by SAAB EDS to much extent. One problem with the valves has been the manual adjustment of the regulating temperature during the production phase. The uncertainty of its temperature intervals, together with an incorrect configuration of the valve settings, has at times prevented the operator room from reaching comfortable temperature for the operators. Another negative effect of this is that other subsystems, that include electronics, will get too cold in comparison to the operator room which could lead to condensed water coming into close contact with the electronics.

In the final ARTHUR product there is no way for the operators to adjust the valve's configuration due to their unreachable location and general safety restrictions. Since it is a necessary function to be able to adjust the operator room temperature, the cooling system has been implemented with a thermostat that can override the valve functionality to increase or

decrease the operator room temperature. Unfortunately, this override function disrupts the control scheme that is based only on valves and it causes oscillations in the systems.

Because ARTHUR is in the process of being updated, it is of utmost importance to investigate the mentioned problems and the reasons behind them. A characterization of the cooling system and its control could increase the knowledge of the product and thereby be helpful when making improvements to it.

1.2 Purpose

The purpose of the project was to describe the cooling system on a system level and create a simulation model, which can be used to find out where improvements can be made to the system. To model the system it was necessary to perform experiments on the AVTA valves in order to characterize their behavior for different temperatures. Further, the simulation results have been compared with real data to evaluate the accuracy of the model.

The purpose of the project has been divided into several steps and it can be used as a rough outline of the work towards a successful final result:

- Describing and characterizing the present cooling system in ARTHUR.
- Investigating the analogue valves (AVTA).
- Modeling and simulating the cooling system.
- Comparing and evaluating the model with real data.
- Discussing and suggesting possible new ways to control the present cooling system.

1.3 Limitations

To be able to create a model that is detailed enough but also keep the complexity on a fair level for a Master of Science thesis, a few limitations are necessary. The Liquid Cooling Unit (LCU) has its own set of control schemes to adjust the cooling power, which results in a certain Ethylene Glycol Water (EGW) temperature output from the LCU. In this report the cooling power is assumed to be constant over time and the lowest possible output temperature from the LCU is 5 ˚C. The description of the LCU will be limited, because a previous Master of Science thesis has already been performed solely on the LCU [1].

The cooling of the operator room's air temperature is credited to the ACU and without simplifications of the ACU's functionality the modeling would become very complex. Therefore, the mass of ARTHUR's cabin and the air inside it will be considered to have the

same temperature and change uniformly, i.e., the air flow will not be modeled. An additional simplification is that the temperature gradient of the cabin will not be considered in the modeling.

It has only been possible to test and investigate the whole ARTHUR system during a very short time period due to availability issues, which has proved to be an involuntary limiting factor of this project.

The simulation scenarios have been limited to hot ambient temperatures, i.e., only cooling mode of the climate system will be modeled. As a consequence, heating of the cabin temperature is not included in the model.

1.4 Method

The work towards an accomplishment of the purpose of the project has been performed mostly in the software MATLAB/Simulink. The literature that has been used to model the climate system in Simulink includes, e.g., [2] for properties of heat exchange in thermodynamic systems and [3] for theory about defining dynamical properties. The literature has been complemented by the know-how of several SAAB EDS employees with long experience from ARTHUR, and by several internal SAAB EDS reports. These internal documents include, e.g., a report on temperature testing of ARTHUR at Sveriges Tekniska Forskningsinstitut [4], and a product specification of the LCU [5].

The focus of the modeling process was on a system level to be able to get an overview of the whole system and the interaction between the subsystems instead of a too detailed description of only a few parts of the system. An exception to this system level focus was the detailed investigation on the AVTA valves. An experimental setup for the valves was used to determine the connection between the valve configuration and its temperature characteristics, the control range of the valves, and the dynamics of the valves.

As a part of the modeling process it was necessary to use previous temperature test data on ARTHUR. The test data from [4] was used to approximate a few unknown constants regarding the heat exchange in the subsystems. Further, to assist in the modeling, a short test with an ARTHUR cabin was completed and this provided useful information on the ACU valve.

The simulation results have been compared with the available test data and thereby the accuracy of the model could be evaluated as well.

1.5 Structure of Report

Section 1 gives an introduction to the project and explains why this report is of interest. Further, the section includes the definition of the purpose and the limitations of the project.

Section 2 presents an overview of the cooling system, describes each subsystem and its functions, and explains the type of control used in the cooling system.

Section 3 describes the experiments performed on the valves and also presents the results from them. This section also presents results from previous experiments at SAAB EDS.

Section 4 explains the implementation of the valve dynamics, defines the heat transfer in the different subsystems, and presents additional dynamics in the cooling system.

Section 5 presents the simulation results and compares them with real temperature data of ARTHUR.

Section 6 evaluates the present system and discusses the accuracy of the model. Further, the section gives suggestions of new types of control for the cooling system.

2 Structure of Cooling System

This section will present an explanation of the ground radar and give an overview of the cooling system by describing the subsystems and their functionality.

2.1 Cooling System for Ground Radar

SAAB's ARTHUR, see Figure 2.1, is a mobile ground radar whose task is to seek, intercept and follow projectiles. It can follow a number of projectiles and at the same time continuously search for new ones. From the projectile's orbit ARTHUR can find the location where the enemy's projectile was fired, or alternatively find the location where the ally's projectile struck. ARTHUR can be used in a large interval of ambient temperatures, ranging from -40 ˚C to +55 ˚C. ARTHUR is designed so that it easily can be placed on a truck, thus simplifying the transport and mobility of the cabin which has a mass of approximately 4500 kg.

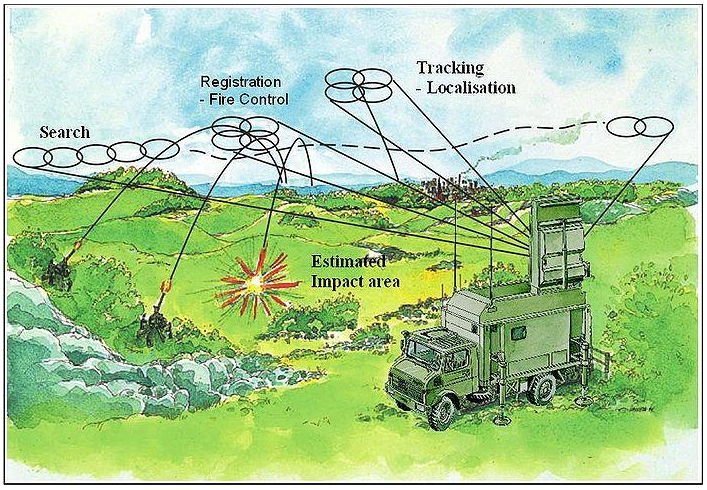

Figure 2.1 Overview of ARTHUR's abilities [6].

To perform its tasks ARTHUR have many components, e.g., a lot of electronics, a travelling wave tube, and two operator seats. To complete the tasks in different ambient temperatures ARTHUR is supplied with a climate system that includes five subsystems and an EGW distribution net, see Figure 2.2 . The five subsystems include an LCU, an ACU, a TWT-CU, an SDU, and a TRU, which will all be further described in the sections that follow.

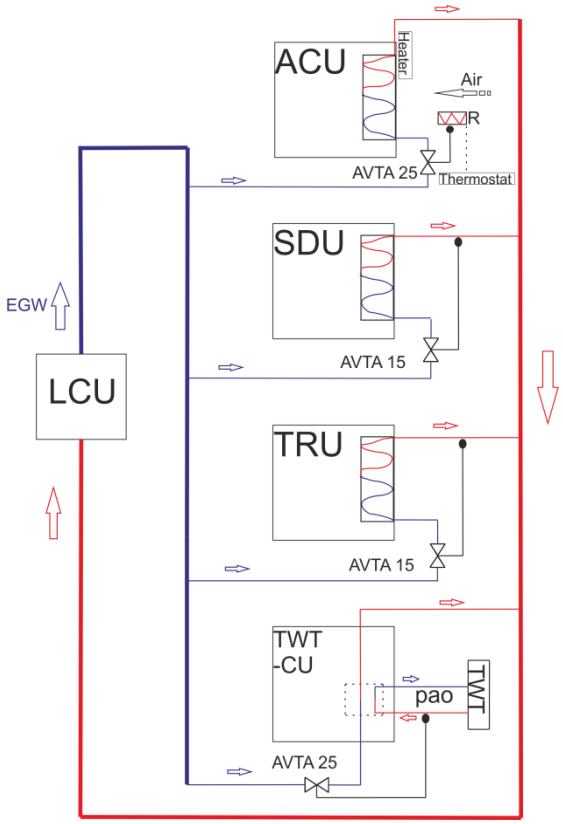

Figure 2.2 Block scheme of climate system.

The LCU cool and distribute the EGW to the different subsystems, which all have some type of heat exchanger located inside. To control the flow into the subsystems, and accordingly control the cooling power, the climate system uses valves with temperature sensors. As can be seen in Figure 2.2 the subsystems have different placements of the temperature sensors, i.e. located at the return EGW for the Transmitter Unite (TRU) and the Signal Data Unit(SDU), at the inlet air for the Air Conditioning Unit (ACU), and at the hot side of the Polyalphaolefin (PAO) for the Travelling Wave Tube-Cooling Unit (TWT-CU).

2.2 Liquid Cooling Unit

The heart of the cooling system is the LCU. It is where the EGW is cooled from hot to cold temperature and pumped out to the distribution net. The LCU has its own set of control schemes to adjust the cooling power, which results in a certain EGW temperature output from the LCU. In this report the cooling power is assumed to be constant over time, 11 kW, and the lowest possible output temperature from the LCU is 5 ˚C.

The LCU consists of three parts: the compressor unit (evaporator heat exchanger, pump, compressor and diverter valve), the condenser unit (condenser heat exchanger and two fans),

and the expansion tank. A schematic view of the LCU can be seen in Figure 2.3, but for more detailed information on the LCU the reader is referred to [1].

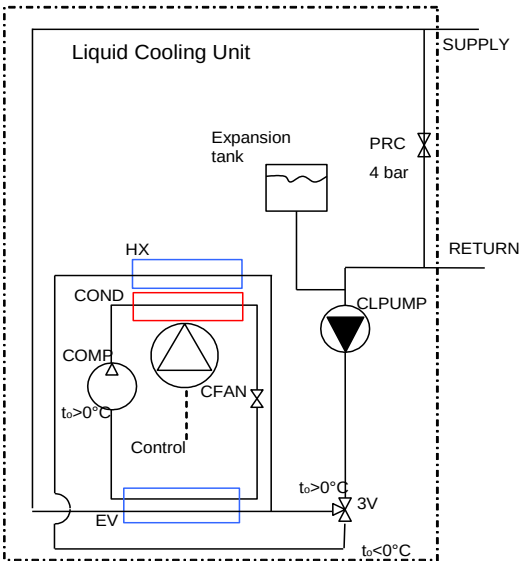

Figure 2.3 Schematic view of the LCU [7].

The output data of the LCU that is available from the supplier is a little shorthanded, therefore a curve fit was performed in MATLAB's Curve Fitting Tool. The pressure-flow characteristics of the LCU can be seen in Figure 2.4 together with the supplier's output data.

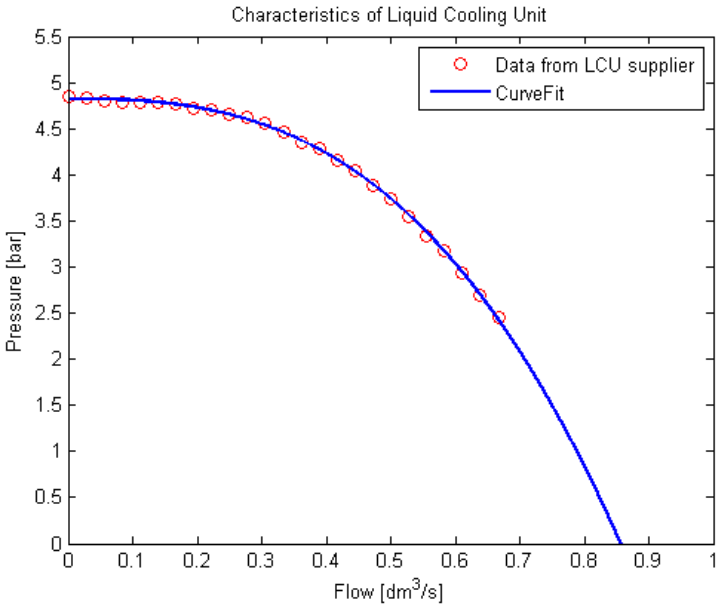

Figure 2.4 Characteristics of the LCU.

Worth noting from the LCU output data is that it does not produce a constant flow, which means that the operating point of the LCU will depend on the opening of the valves. This will

be studied in Section 2.6. Further, as a safety measure, the LCU's maximum differential pressure is limited, $\Delta p_{max} = 4$ bar, with the use of a pressure sensitive valve between the supply and return side of the LCU.

2.3 Air Conditioning Unit

The ACU produce cold air to the operator room with the use of a heat exchanger that is large compared to the ones in the other subsystems. To cool the operator room it is required that the cooling power is larger than the heating power. Simplified, the heating power can be viewed as the summation of the transferred heat from the ambient air and the heat coming from the operators inside the cabin.

As seen in Figure 2.2, the temperature sensor is located at the air inlet of the ACU and it is connected to a large valve. Unfortunately, there is no way for the operators to adjust the valve's configuration due to their unreachable location, thus preventing the possibility to change the air temperature. Therefore, a thermostat linked to a resistance has been implemented which can override the valve's temperature sensor. During cooling mode the thermostat works as an ON/OFF switch which can initiate current to be run through a resistance. The resistance is located next to the valve sensor and will largely influence the sensor temperature. Depending on if the thermostat sensor temperature is above or below the thermostat set point, the resistance is active (ON) or inactive (OFF), respectively.

The idea behind the ON state is that it should result in a sensor temperature that will open the ACU valve as much as possible and consequently give the largest possible flow into the ACU. This relationship will be studied further in Section 3.1.1 and 3.2, with respect to the properties of the valves and the resistance. The thermostat unfortunately does not provide optimal comfort for the operators, largely due to the fact that the ACU system will have a slow regulation, but also due to the oscillations which is a side effect of the override function.

2.4 Signal Data Unit and Transmitter Unit

The SDU and the TRU are two units that have different functionality in regards to the whole radar system, but they are very similar in a modeling perspective in this report. A simplified description of the units is that they are a combination of electronics, where the TRU is involved in the transmission out from the TWT while the SDU has its focus on signal processing. The mass, 50 kg, and the size of the heat exchanger can be treated as equal for the

SDU and the TRU. Unlike the ACU's unknown cooling power consumption, the SDU's and the TRU's electronics have a well defined power consumption of 400 watt. The similarity also holds for the placement of the valve's sensor which is located at the return side of the EGW, see Figure 2.2.

2.5 Travelling Wave Tube – Cooling Unit

The TWT-CU's task is to cool the wave tube where the radar signal of 4 kW is sent out from. The wave tube is temperature sensitive so it is important that it is kept within the safety margins. The liquid that is used to cool the wave tube is a synthetic oil called PAO, which is commonly used as radar coolant [8]. The PAO is pumped though a separate pipe-loop with a constant flow of 10 liter/min [9]. The PAO is in turn cooled by the EGW. The placement of the valve's sensor for the TWT-CU is at the hot side of the PAO loop, see Figure 2.2.

2.6 AVTA Valves and Operating Point of Cooling System

The AVTA valve is a type of P-regulator that will open its valve cone proportionally according to a change in temperature. A sketch of the AVTA valve can be seen in Figure 2.5.

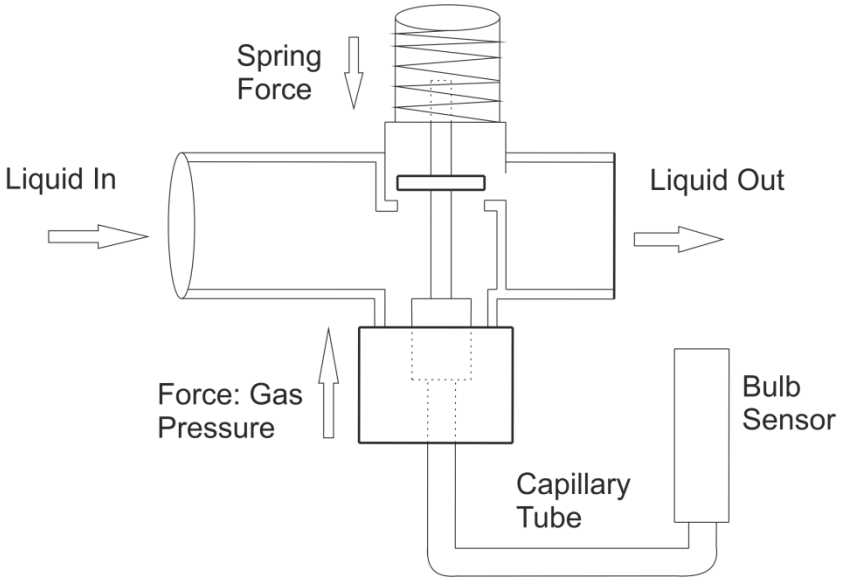

Figure 2.5 Sketch of the AVTA valve and the two forces present.

The AVTA valve uses a hermetically sealed thermostatic element with a sensor bulb, capillary tube and bellows. The sensor bulb contains an adsorption charge (a vapor charge)

that produces pressure changes in the element dependent on temperature changes [10]. The pressure is transferred via the capillary tube and bellows to finally act as a force on the valve. The force acts on the valve and tries to open or close it. Located on the opposite side of the valve is a mechanical spring, which generates a force acting in the opposite direction of the bellows. The size of the spring's force depends on the spring's stiffness, which can be manually configured with a knob at the top of the valve.

A more uncertain force that could possibly affect the valve is the force that originates from the pressure in the EGW. The EGW force would then act in the opposite direction of the spring. The quantity of this force is very hard to find but it is so low that it can be assumed to not have a significant impact of the resulting valve opening [11].

The proportional control that the valves utilize at a specific temperature depends on the stiffness configuration of the AVTA spring. The default spring configuration and the size of the different subsystems' valves are presented in Table 2.1. The configuration of the spring, with nominal scale 1-5, will result in a temperature where the valve will start to open and where it will close, thereby defining the temperature interval for that configuration. These temperature characteristics are unfortunately not available in any documentation neither from the supplier nor from SAAB EDS, and it is therefore focused on in Section 3.1.

Subsystem	**Default Spring Configuration (1-5)**	**Valve Size**	
		Name	**Connection**
ACU	2.7	AVTA 25	1 inch
TWT-CU	2.0	AVTA 25	1 inch
SDU	1.5	AVTA 15	0.5 inch
TRU	2.0	AVTA 15	0.5 inch

Table 2.1 Default spring configuration and valve size

The sensor temperature together with the spring configuration will be the two deciding quantities that result in an opening area of the valve. According to [12], the opening area can also be viewed as a coefficient, K_v, which relates the valve's pressure drop, Δp, to the flow through it, q, by the following relationship:

$$q = K_v \sqrt{\Delta p} \quad \textbf{(1)}$$

Thus, the K_v value modifies the slope of the valve's pressure-flow characteristics. The K_v value implicitly depends on the size of the valve, e.g., the valve is larger in the ACU than in the other subsystems and as a result it is possible to achieve a larger flow compared to the smaller valves used.

The pipes in the EGW distribution net are dimensioned in such a way that the subsystems can theoretically be considered to be connected in parallel, which means that there is no pressure drop in the pipes. From this fact it is straightforward, using the theory of parallel connections, to point out that the differential pressure over respective AVTA valve is approximately equal. Assuming a known K_v value for each valve it is now possible to sum each valve's flow that corresponds to a specific differential pressure according to:

$$\sum_{i=1}^{4} q_i = K_{v_{tot}} \sqrt{\Delta p} \tag{2}$$

The relationship is shown in Figure 2.6 as well.

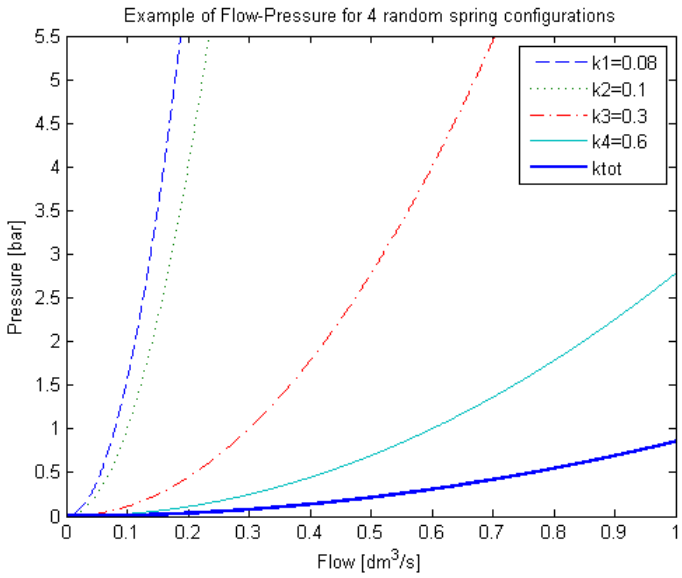

Figure 2.6 An example of four spring configurations and their resulting total curve.

With the four valves' total flow-pressure characteristics it is possible, together with the LCU flow-pressure characteristics, to find the operating point of the cooling system. The intersection between the two curves defines the operating point of the cooling system, see Figure 2.7 with randomly chosen K_v values for an example of a possible situation. The dynamical property of the cooling system causes the operating point to change with time depending on the valves' K_v values.

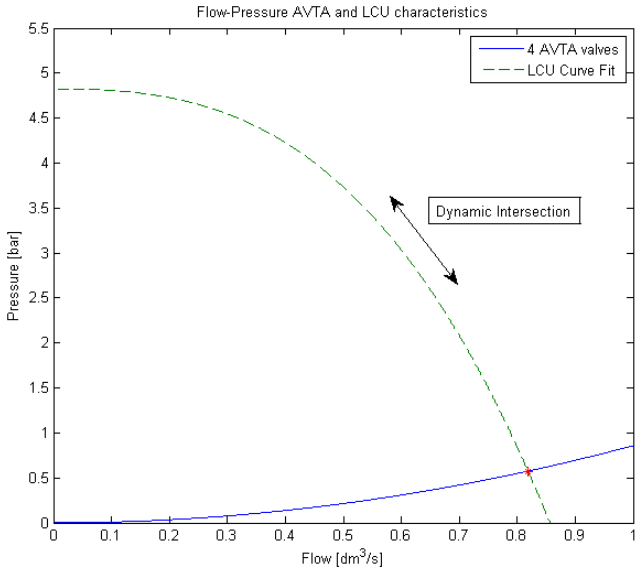

Figure 2.7 Dynamic intersection of LCU and AVTA valves.

3 Experiments and Data Collection

This section will describe a measuring setup and present the results from experiments performed. This section will also present data from previous testing performed at SAAB EDS.

3.1 AVTA Valve

The AVTA valve's characteristics are of course of interest and, therefore, a couple of experiments have been performed. The valve and its temperature sensor have been investigated regarding opening and closing temperatures and also how the spring configuration affects the temperature intervals as well as the valve opening size. The measuring setup that was used for the experiments is shown in Figure 3.1. To find the valve opening size for different temperatures, the K_v value, the flow through the valve was measured at three different levels of pressure.

The dynamics of the valve will be the focus of Section 3.1.2. From a brief test run of the AVTA 15 valve it appeared as the valve did not close as fast as it could open. This phenomenon is brought to attention and studied using a positive and negative temperature step applied to the valve.

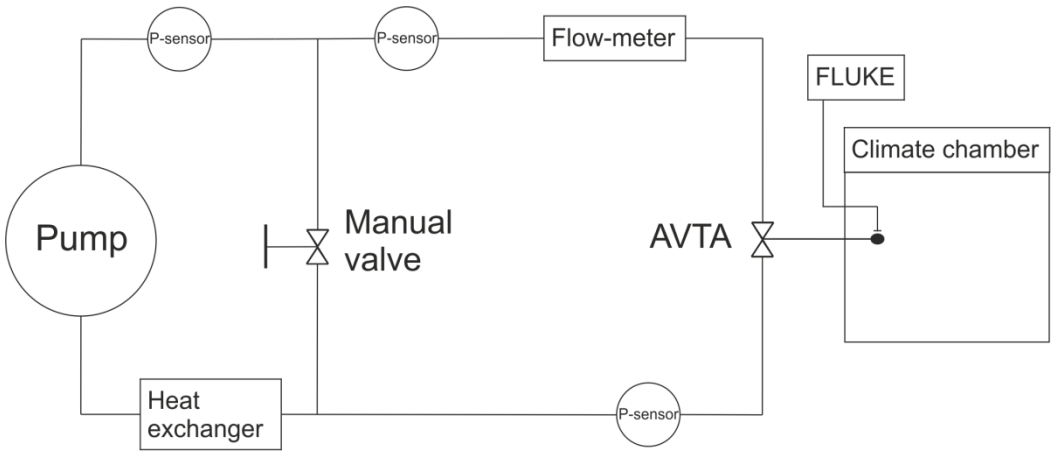

Figure 3.1 Sketch of measuring setup.

As seen from Figure 3.1, the differential pressure over the valve was adjusted with a manual valve to appoint the three different pressures to be able to characterize the valve. With

this setup it was assumed that the pressure drop over the flow meter was negligible. The following instruments were used at the experiments:

- AVTA valve size 15 or 25. Analogue valves from Danfoss.
- Analogue pressure sensor. Hydroscand with pressure range 0-10 bar.
- Flow meter. Enermet. 9V-MP115.
- Temperature sensor. Fluke 52 K/J Thermometer.
- Climate chamber. Vötsch Industritechnik. VT 4004.
- Water pump. GRUNDFOS CR1-12.
- Heat exchanger. Svenska Fläkt QLED-14-02-4-X.

The cooling system uses two different sizes of the AVTA valve and both have been studied through experiments. The measuring setup was the same for both sizes of the AVTA valve.

3.1.1 Spring Configuration and Temperature Influence on K_v

With a temperature increment of 2 ˚C in the climate chamber, the flow through the valve was registered to find two important properties of the valve, namely the valve's temperature interval and the K_v value of each specific temperature.

3.1.1.1 AVTA 15

The results from experiments on the smaller valve, AVTA 15, are presented below. The opening temperature and fully open temperature for different spring configurations are shown in Table 3.1.

Spring Configuration	Opening Temperature [˚C]	Fully Open Temperature [˚C]
0.5	7	31
1.0	23	43
1.5	33	51
2.0	43	63
2.5	53	73
3.0	63	83
3.5	73	95

Table 3.1 Temperature properties of AVTA 15.

From Table 3.1 it is worth noting that an increase in spring configuration of 0.5 will approximately increase the opening temperature of 10 ˚C and consequently increase the temperature where the valve is fully open.

Using the measuring setup described in Figure 3.1 the flow has been measured at three different pressures to find the characteristics of the valve. This was performed for the spring configurations defined in Table 3.1, with a temperature increment of 2 ˚C. From these three data points it is possible, using the Curve Fit Tool in MATLAB, to find the K_v value at every temperature increment. The curve fitting have been performed to fit the relationship according to Equation (1), i.e.

$$\Delta p = \frac{q^2}{{K_v}^2} \tag{3}$$

The result of the curve fitting will be an approximation of the valve's characteristics and it will provide sufficient information to model the valve in this project. In Figure 3.2 a curve fitting is shown for the AVTA 15 with a spring configuration of 1.0.

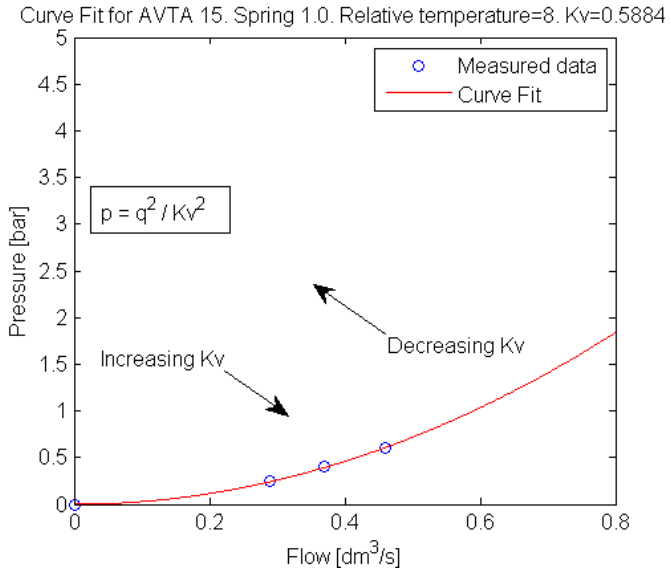

Figure 3.2 Curve fit for AVTA 15 with spring configuration 1.0.

An analysis of all the curve fitting results shows that the K_v value for each spring configuration is very similar for the same relative temperature (with respect to the opening temperature). Since the characteristics of the K_v value does not depend on the spring configuration, an average of the K_v value was calculated for each relative temperature and is shown in Table 3.2.

Relative Temperature [˚C]	K_v Value
0	0.02
2	0.0707
4	0.2063
6	0.5114
8	0.7220
10	0.8405
12	0.9130
14	0.9481
16	0.9760
18	1.0006
20	1.0095

Table 3.2 Valve opening size for AVTA 15.

From Table 3.2 one can conclude that the K_v value increases quite a lot in the mid-range of the relative temperature interval and not as much for the high-range temperature interval.

3.1.1.2 AVTA 25

The results from experiments on the larger valve, AVTA 25, are presented below. The opening temperature and fully open temperature for different spring configurations are shown in Table 3.3.

Spring Configuration	Opening Temperature [˚C]	Fully Open Temperature [˚C]
1.0	0	20
2.0	20	40
3.0	40	60

Table 3.3 Temperature properties of AVTA 25.

It is clear from Table 3.3 that the opening temperatures for the AVTA 25 valve are different compared to the AVTA 15 valve. This could not be discovered from AVTA's datasheets and therefore these results are important for a correct modeling of the cooling system.

The same measuring setup and method as in Section 3.1.1.1 have been used in the experiments for the AVTA 25 valve, therefore the results will be presented here without further repetitive descriptions. An analysis of all the curve fitting results shows that the K_v value for each spring configuration is very similar for the same relative temperature.

Therefore an average of the K_v value was calculated and the relationship between the relative temperature and the K_v value is shown in Table 3.4.

Relative Temperature [˚C]	**K_v Value**
0	0.0133
2	0.0333
4	0.1676
6	0.3736
8	0.5884
10	0.8601
12	0.9998
14	1.0966
16	1.1428
18	1.2017
20	1.2300

Table 3.4 Valve opening size for AVTA 25.

The valve opening size for AVTA 25, K_v, logically has a larger maximum value compared to AVTA 15.

3.1.2 Valve Dynamics

One way to gain understanding of the unknown dynamic interaction of the valve's bulb temperature and pressure build-up from the adsorption gas, in connection with the resulting possible flow through the valve, was to measure the flow through the valve during a temperature step input to the valve. Since the relationship between flow and temperature is known, via the K_v value, the measured flow and pressure can be used to find the corresponding bulb temperature. Consequently, the temperature step response can be observed.

The temperature step was in the form of an increase or decrease of 20˚C in the climate chamber. The same experiment was performed for the AVTA 15 valve and the AVTA 25 valve. It was also investigated if the different spring configurations had any effect on the characteristics and time constants of the valve.

Almost the same measuring setup as in Figure 3.1 was used, with the exception being that two climate chambers were used instead of only one. A temperature step was applied to the valves by quickly moving the bulb sensor between the two climate chambers to minimize the influence of the room's air temperature on the bulb sensor.

3.1.2.1 AVTA 15

From a previous experiment, see Section 3.1.1.1, it was known at what temperature interval the AVTA 15 valve will be active and therefore temperature steps were applied according to Table 3.5.

Spring Configuration	Positive Temperature Step [˚C]	Negative Temperature Step [˚C]
1.0	23 → 43	43 → 23
2.0	43 → 63	63 → 43
3.0	63 → 83	83 → 63

Table 3.5 Description of temperature step applied to AVTA 15 valve.

The positive step responses for the AVTA 15 valve, with an increase in temperature, are shown in Figure 3.3, Figure 3.4 and Figure 3.5. In the figures one can see that the step response does not reach the temperature level of 20˚C and the most likely reason for this is the uncertainty in the manual setting of the AVTA valve's pressure. If the pressure was too low it would show up as a problem when the maximum flow was measured, which via the K_v value gives a step response that does not reach the relative temperature of 20 ˚C.

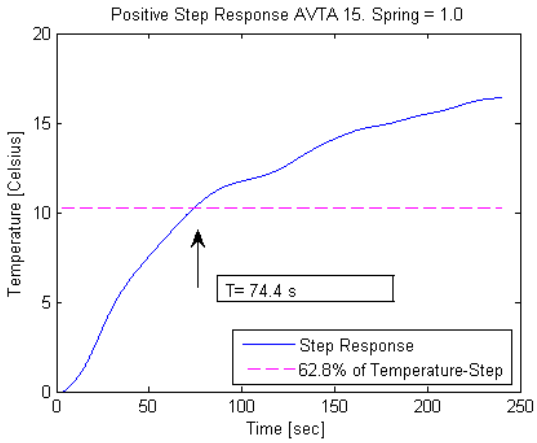

Figure 3.3 Positive step response AVTA 15. Spring 1.0.

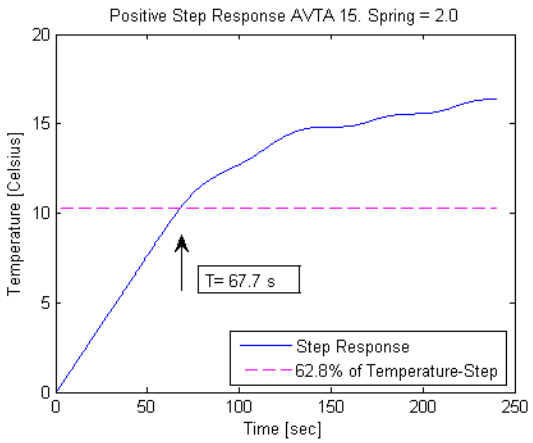

Figure 3.4 Positive step response AVTA 15. Spring 2.0.

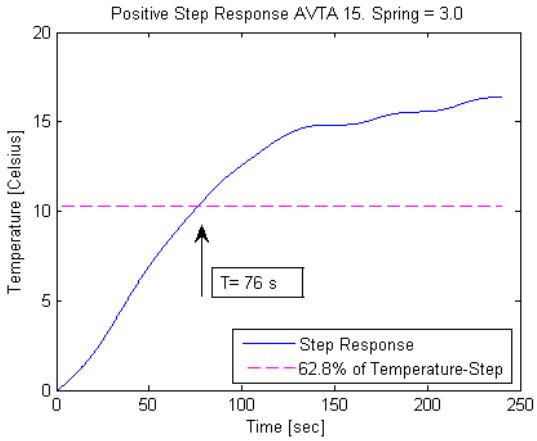

Figure 3.5 Positive step response AVTA 15. Spring 3.0.

The positive step responses of the AVTA 15 valve resemble a step response of a first order system. For a first order system the time constant is the time it takes for the step response to reach ~ 63 % of its final value [3]. The time constant for the valves, assuming first order systems, is pointed out in Figure 3.3, Figure 3.4 and Figure 3.5 and are all summarized in Table 3.6.

Spring Configuration	Time Constant [sec]
1.0	74
2.0	68
3.0	76

Table 3.6 Positive time constants for AVTA 15.

The time constants are in the neighborhood of each other and from these results it is hard to conclude that the time constant would depend on the spring configuration.

As for the negative step responses, it is clear from Figure 3.6, Figure 3.7 and Figure 3.8 that the time constants are rather much longer in comparison to the positive step responses. One reason for this could be that the adsorption gas inside the sensor bulb has different time constants for when the gas pressure increases and decreases. However, this will not be investigated further in this report.

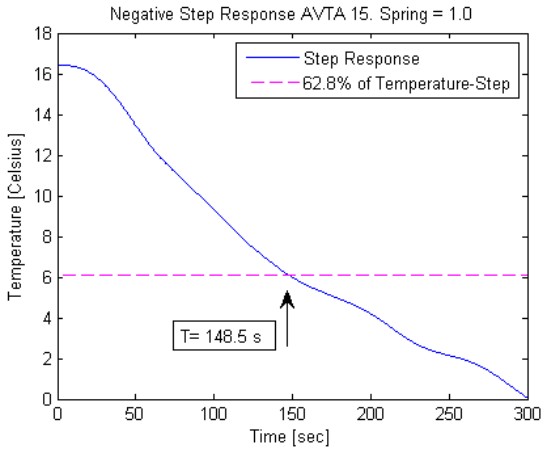

Figure 3.6 Negative step response AVTA 15. Spring 1.0.

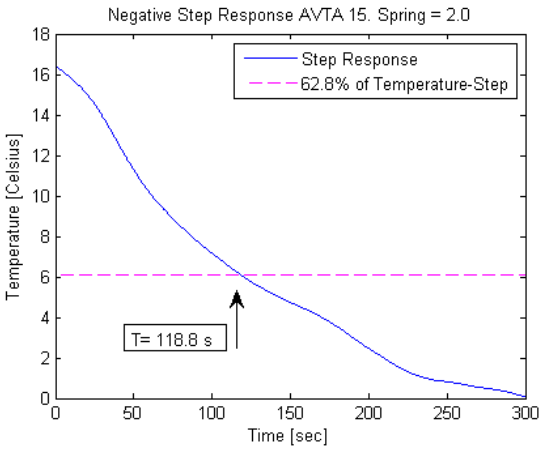

Figure 3.7 Negative step response AVTA 15. Spring 2.0.

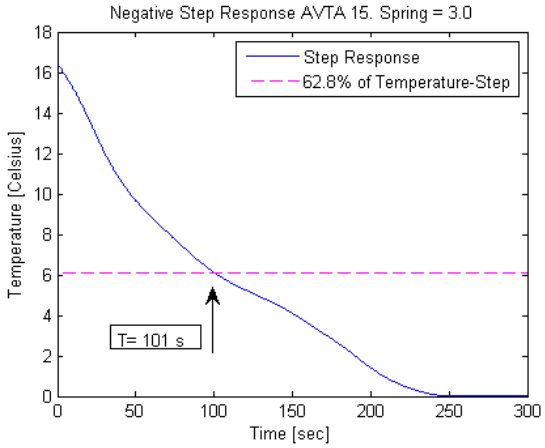

Figure 3.8 Negative step response AVTA 15. Spring 3.0.

The time constant for the valves are pointed out in Figure 3.6, Figure 3.7 and Figure 3.8 and are all summarized in Table 3.7 below. The step response that resembles a first order system the most is the step response of the valve with spring configuration 3.0, see Figure 3.8.

Spring Configuration	Time Constant [sec]
1.0	149
2.0	119
3.0	101

Table 3.7 Negative time constants for AVTA 15.

From Table 3.7 one should note that the time constant decreases when the valve has a higher spring configuration.

3.1.2.2 AVTA 25

From a previous experiment, see Section 3.1.1.2, it was known at what temperature interval the AVTA 25 valve will be active and therefore a temperature step was applied according to Table 3.8.

Spring Configuration	Positive Temperature Step [˚C]	Negative Temperature Step [˚C]
1.0	0 → 20	20 → 0
2.0	20 → 40	40 → 20
3.0	40 → 60	60 → 40

Table 3.8 Description of temperature step applied to AVTA 25 valve.

The positive step responses for the AVTA 25 valve, with an increase in temperature, are shown in Figure 3.9, Figure 3.10 and Figure 3.11. In Figure 3.11 a problem arises, where the step response does not reach the temperature level of 20˚C. As for the AVTA 15 valve, if the valve pressure was too low it would show up as a problem when the maximum flow was measured and result in a step response that does not reach the relative temperature of 20 ˚C.

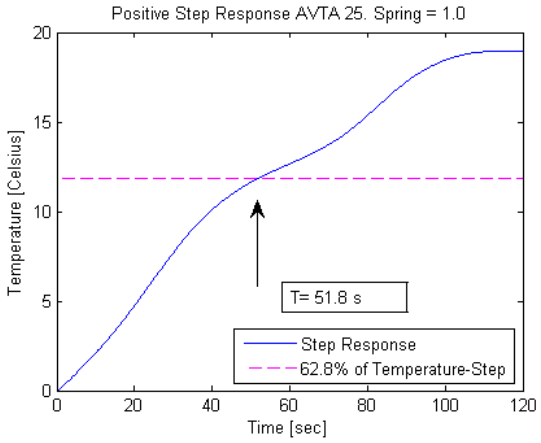

Figure 3.9 Positive step response AVTA 25. Spring 1.0.

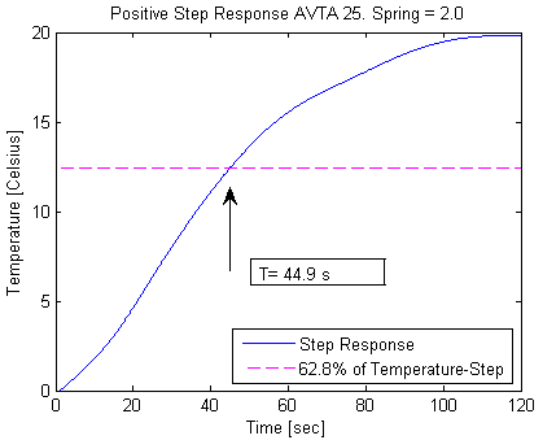

Figure 3.10 Positive step response AVTA 25. Spring 2.0.

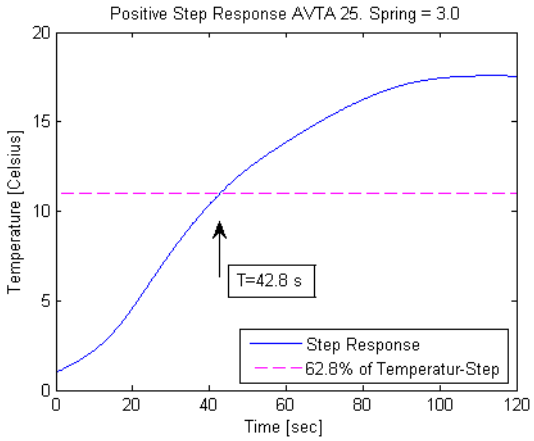

Figure 3.11 Positive step response AVTA 25. Spring 3.0.

The time constants for the AVTA 25 valve, assuming first order systems, are pointed out in Figure 3.9, Figure 3.10 and Figure 3.11 and are all summarized in Table 3.9 below.

Spring Configuration	Time Constant [sec]
1.0	52
2.0	45
3.0	43

Table 3.9 Positive time constants for AVTA 25.

The time constants are in the neighborhood of each other but there is a small trend towards shorter time constant for an increasing spring configuration.

As for the negative step responses it is clear from Figure 3.12, Figure 3.13 and Figure 3.14 that the time constants are longer in comparison to the positive step responses. Further, from Table 3.10 one can note that the time constant decreases when the valve has a higher spring configuration.

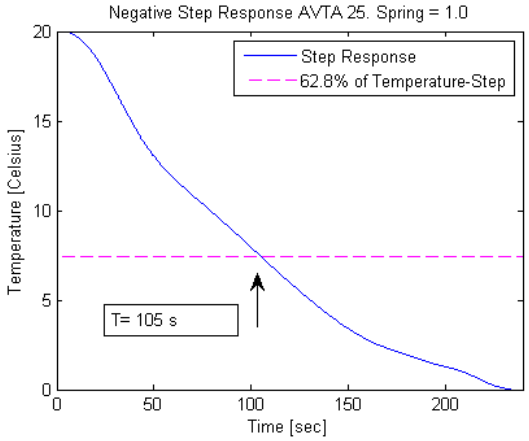

Figure 3.12 Negative step response AVTA 25. Spring 1.0.

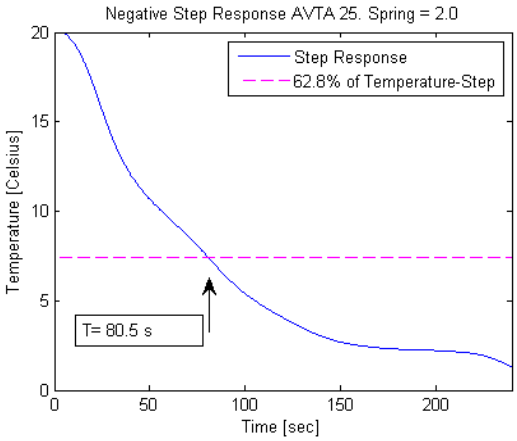

Figure 3.13 Negative step response AVTA 25. Spring 2.0.

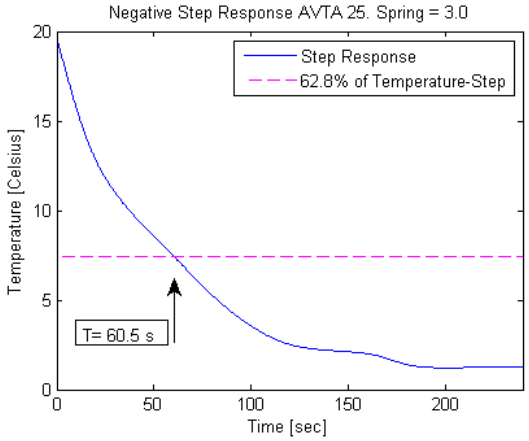

Figure 3.14 Negative step response AVTA 25. Spring 3.0.

Spring Configuration	Time Constant [sec]
1.0	105
2.0	81
3.0	61

Table 3.10 Negative time constants for AVTA 25

3.2 ARTHUR Test

A short test was performed on an ARTHUR module during the time frame of this project. The objective of the test for SAAB EDS was to make sure that the AVTA valves were configured correctly. Unfortunately, the test was performed in room temperature at the SAAB EDS facility in Kallebäck and therefore the usage of the test results was limited for this report.

However, temperature data of the ACU's resistance was collected and Figure 3.15 shows the resistance during a warm up as the ACU's override function has been switched ON.

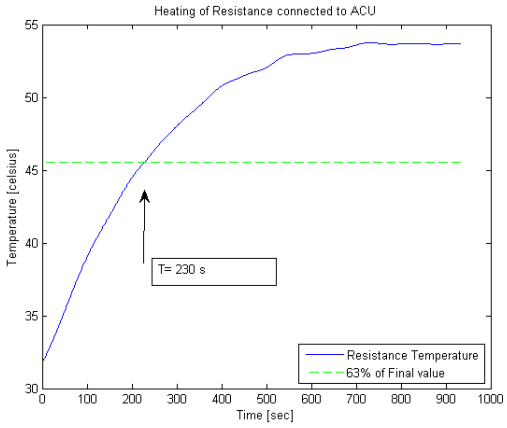

Figure 3.15 Heating of the ACU's resistance.

The ACU's resistance has the characteristics of a first order system and it has a maximum temperature, $T_{Resistance,max} = 53$ ˚C . In Figure 3.15 the time constant, assuming a first order system, is pointed out to be $\tau_{Resistance} = 230\ sec$.

3.3 Temperature Data of ARTHUR from SP Testing

For SAAB EDS to be able to test and verify the full capacity of ARTHUR it is necessary to use a large climate chamber that can simulate different extreme ambient temperatures. For such tests, SAAB EDS use the climate chamber at SP's testing facility in Borås, Sweden. During the time frame of this project there has not been any testing of ARTHUR at SP, therefore earlier test results from May 2011 will be used. The data collection will be based on a test run from [4], where the simulated ambient temperature was 55 ˚C. The data will assist in this report's modeling process and also as a part of the validation of the simulation model. During the SP test temperature sensors were placed at appropriate locations inside ARTHUR, e.g., at the air inlet of the ACU, and at the EGW inlet and outlet to every subsystem. Temperature data series for the ACU, the SDU, the TRU and the TWT-CU are presented in Figure 3.16, Figure 3.17, Figure 3.18, and Figure 3.19 respectively.

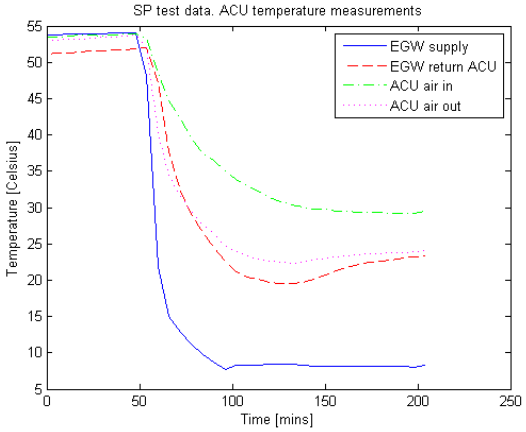

Figure 3.16 ACU temperature measurements from SP.

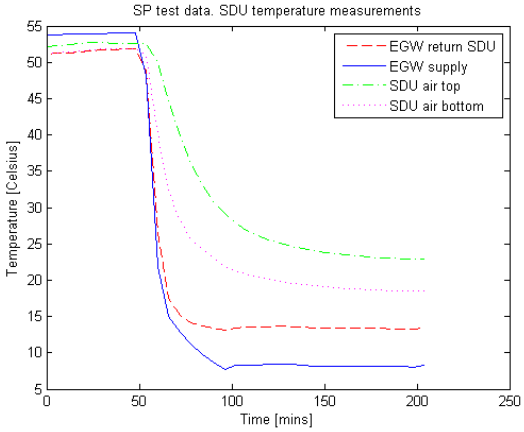

Figure 3.17 SDU temperature measurements from SP.

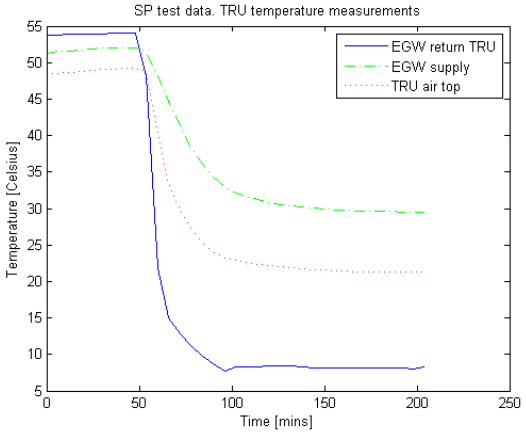

Figure 3.18 TRU temperature measurements from SP.

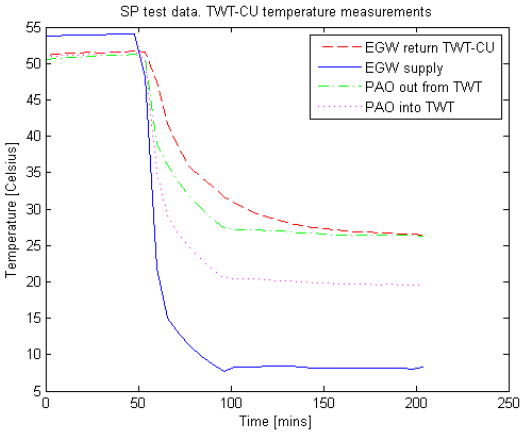

Figure 3.19 TWT-CU temperature measurements from SP.

The temperature measurements show that all parts of ARTHUR are initially ~50-55 ˚C and that after 48 minutes the cooling system is started. The LCU can cool the EGW supply in about 50 minutes and it stabilizes at approximately 8 ˚C. From Figure 3.16 it is clear that the ACU air inlet temperature stabilizes at approximately 29 ˚C after about 155 minutes. The time for the other subsystems to reach steady state temperatures is very similar to the ACU, which is logical because the ACU performance will influence the whole cabin's temperature. However, one should note that the SDU has a lower steady state temperature, 23 ˚C, so it is not only the ACU performance that depicts the subsystem's temperature.

By comparing the characteristics of the EGW return temperature it is clear that the ACU and the TWT-CU will increase the EGW temperature much more than the SDU and the TRU, which is the consequence of a much larger heating power present in the ACU and the TWT-

CU. A summary of the steady state temperatures is presented in Table 3.11. Note that the SP data for the EGW TRU return was corrupt and therefore not presented.

Sensor location	**Temperature [˚C]**
EGW LCU supply	8.2
EGW LCU return	11.5
ACU air in	29.6
ACU air out	24.1
EGW ACU return	23.4
SDU air top	22.9
SDU air bottom	18.5
EGW SDU return	13.4
TRU air top	29.5
TRU air bottom	21.3
EGW TRU return	Corrupt
EGW TWT-CU return	26.4
PAO into TWT	19.6
PAO out from TWT	26.3

Table 3.11 Sensor temperatures at SP test after ~155 minutes

From these temperature data series it is possible to point out a problem with the cooling system. The problem is that the ACU air temperature is quite high, 29 ˚C, which means that it does not provide very good comfort for the operators inside the cabin. SAAB EDS expects a temperature, according to the default spring configuration of the ACU's valve, of at the most 25 ˚C. Unfortunately, as experiments on the AVTA valves have shown this is not a correct expectation to have if the valve's spring has been configured incorrectly. At a continued testing at SP the spring configuration of the ACU's valve was lowered and that resulted in a lower ACU temperature, see Figure 3.20.

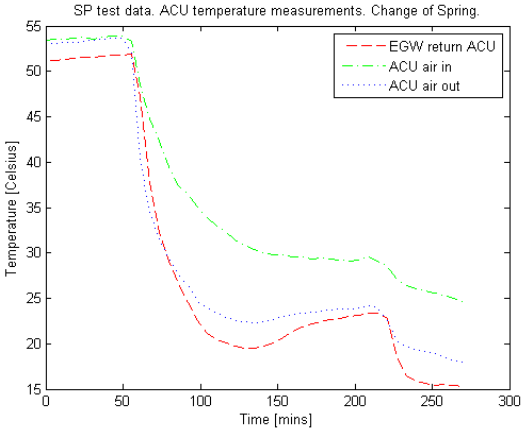

Figure 3.20 ACU temperature measurements from SP. ACU valve configuration was changed after 220 minutes.

4 Modeling of Cooling System

In this section the cooling system will be described in more detail with regards to the modeling process. Some parts of the implementation in MATLAB/Simulink are also described in this section.

4.1 Valve Dynamics and K_v Value

The information from Section 3.1 on the AVTA valves (relationship between spring configuration, temperature interval and K_v value) makes it possible to implement blocks and lookup tables in Simulink that describes the characteristics of the valves for different temperatures. A user input of a spring configuration defines the opening temperature for the valve which results in a temperature interval where control can be executed. Every subsystem will simulate a temperature that acts as the AVTA sensor reading. The simulated sensor reading results in an opening size, K_v value, of all the valves. The K_v values for the four valves results in a total flow-pressure curve for the four valves together. The intersection of this curve and the LCU flow-pressure curve results in the operating point of the cooling system. Hence, a theoretical EGW flow is known which is necessary to model the heat transfer in the different subsystems.

The dynamics of the valves are implemented as first order systems using Simulink's block for transfer functions. Since the valves have different time constants depending on the sign of the temperature derivative, a switch was implemented to change between respective time constants depending on the temperature derivative.

4.2 Heat Transfer in Subsystems

The heat transfer for a heat exchanger can be described according to [2]:

$$Q = k\ A\ \Delta T_{am} \tag{4}$$

where ΔT_{am} is given by the temperature differences on the hot and cold side of the heat exchanger, according to

$$\Delta T_{am} = \frac{\left(T_{hot,in} + T_{hot,out}\right)}{2} - \frac{\left(T_{cold,in} + T_{cold,out}\right)}{2} \tag{5}$$

Further, from [2] or [13] the heat that is transferred from the cooling liquid flow can be described according to:

$$Q = \dot{m}\, C_p\, (T_{in} - T_{out}) \tag{6}$$

Now, using Equation (4) and Equation (6) the heat balance for the different subsystems can be stated. The heat balance for the ACU subsystem, which is supposed to cool the operators, the mass of the cabin and the air inside of it, can be described in the following way:

$$\underbrace{\frac{d}{dt}\left(Q_{ACU_{int}}(t)\right)}_{\substack{Derivative\ of \\ Internal \\ Energy}} = \underbrace{k_{cabin}\left(T_{ambient} - T_{ACU}(t)\right)}_{\substack{Heating\ power \\ from\ outside \\ cabin}} + \underbrace{Q_{op}}_{\substack{Heating\ power \\ from \\ operators}} + \underbrace{\dot{m}(t)\, C_{p,egw}\left(T_{c,in}(t) - T_{c,out}(t)\right)}_{\substack{Cooling\ power \\ from \\ EGW}} \tag{7}$$

The heat balance in Equation (7) is based on the assumption that the temperature of the cabin and the air inside of it is uniform. The approach with a uniform temperature, $T_{ACU}(t)$, unfortunately means that the model cannot describe the temperature gradient of the air and the cabin.

The cooling power of the ACU can also be viewed as the difference in air and EGW temperature in the heat exchanger as follows:

$$\dot{m}(t)\, C_{p,egw}\left(T_{c,in}(t) - T_{c,out}(t)\right) = -k_{hx,ACU}\left(T_{ACU}(t) - \tilde{T}_{c,ACU}(t)\right) \tag{8}$$

where $\tilde{T}_{c,ACU}(t)$ is the average temperature of the EGW in the heat exchanger according to:

$$\tilde{T}_{c,ACU}(t) = \frac{T_{c,in}(t) + T_{c,ACUout}(t)}{2} \tag{9}$$

Now, Equation (7) can be written in the following way:

$$\frac{d}{dt}\left(C_{p,ACU}\, m_{ACU}\, T_{ACU}(t)\right) = k_{cabin}\left(T_{ambient} - T_{ACU}(t)\right) + Q_{op} - k_{hx,ACU}\left(T_{ACU}(t) - \tilde{T}_{c,ACU}(t)\right) \tag{10}$$

where the coefficients $k_{hx,ACU}$ and k_{cabin} include the area of the heat exchanger and of the cabin respectively. In Equation (10) the specific heat capacity, $C_{p,ACU}$, and the mass, m_{ACU}, are assumed to be constant.

Now, the same method can be applied to the SDU, the TRU and the TWT-CU with some small changes. For example, it is not the ambient temperature that heats the mass of the SDU box and the TRU box; it is the operator room temperature. The temperature of the TRU

and the SDU is also assumed to be uniform for the subsystem. The heat balance for the SDU can be described according to:

$$\frac{d}{dt}\left(C_{p,SDU}\, m_{SDU}\, T_{SDU}(t)\right) = k_{SDU}\,(T_{ACU}(t) - T_{SDU}(t)) + Q_{SDU,electronics} - k_{hx,SDU}\left(T_{SDU}(t) - \tilde{T}_{c,SDU}(t)\right) \quad \textbf{(11)}$$

where the coefficients $k_{hx,SDU}$ and k_{SDU} include the area of the heat exchanger and of the SDU box respectively. In Equation (11) $C_{p,SDU}$ and m_{SDU} are assumed to be constant. The heat balance for the TRU can be described according to:

$$\frac{d}{dt}\left(C_{p,TRU}\, m_{TRU}\, T_{TRU}(t)\right) = k_{TRU}\,(T_{ACU}(t) - T_{TRU}(t)) + Q_{TRU,electronics} - k_{hx,TRU}\left(T_{TRU}(t) - \tilde{T}_{c,TRU}(t)\right) \quad \textbf{(12)}$$

where the coefficients $k_{hx,TRU}$ and k_{TRU} include the area of the heat exchanger and of the TRU box, respectively.

In the TWT-CU most of the heating power originates from the radar power and it is the PAO that is directly affected by the heating power.

$$\frac{d}{dt}\left(C_{p,PAO}\, m_{PAO}\, \tilde{T}_{PAO}(t)\right) = \overbrace{k_{TWT-CU}\left(T_{ACU}(t) - \tilde{T}_{PAO}(t)\right)}^{small\ influence} + Q_{TWT,radar} - k_{hx,TWT}\left(\tilde{T}_{PAO}(t) - \tilde{T}_{c,TWT-CU}(t)\right) \quad \textbf{(13)}$$

The design of the TWT-CU is such that the heat transfer between the EGW and the PAO takes place at a location inside the TWT-CU where the cabin temperature has a small influence on the PAO. Therefore, in this model, the heating power from the cabin is assumed to be zero.

The temperature data from Section 3.3 can be used to find the steady state relationship of the subsystems' heat balance. Unfortunately, the heat transfer coefficients are unknown for the subsystems. To be able to model the cooling system it is necessary to make approximations of the heating power of the subsystems. It is known that the LCU is somewhat over-sized and this fact is used to approximate the heating power in the following way:

$$Q_{total} = Q_{TWT_{ss}} + Q_{ACU_{ss}} + Q_{TRU_{ss}} + Q_{SDU_{ss}} = Q_{LCU} \leq 11\ kW \quad \textbf{(14)}$$

where $Q_{TWT_{ss}}$, $Q_{ACU_{ss}}$, $Q_{TRU_{ss}}$ and $Q_{SDU_{ss}}$ are the total heating power at steady state in respective subsystem according to Equations (10), (11), (12) and (13). Assumptions are made to satisfy Equation (14) according to:

$$Q_{total} = 4000 + (3600 + 300) + Q_{TRU_{ss}} + 750 \leq 11\,000\ [\mathrm{w}] \quad \textbf{(15)}$$

where $Q_{TRU_{ss}}$ can be found later by using the knowledge that the TRU's heat exchanger is very similar to the SDU's heat exchanger.

At steady state, using an average ACU temperature, Equation (10) becomes:

$$\frac{d}{dt}\left(Q_{ACU_{int}}(t)\right) = 0 \Rightarrow$$

$$0 = k_{cabin}\left(T_{ambient} - \tilde{T}_{ACU}(t)\right) + Q_{op} - k_{hx,ACU}\left(\tilde{T}_{ACU}(t) - \tilde{T}_{c,ACU}(t)\right) \quad \textbf{(16)}$$

where the average temperature of the ACU air, $\tilde{T}_{ACU}$, will be used from Section 3.3. With the assumption from Equation (15) together with the SP data from Table 3.11 it is possible to find the heat transfer coefficients according to:

$$k_{hx,ACU} = \frac{Q_{ACU_{ss}}}{\tilde{T}_{ACU} - \tilde{T}_{c,ACU}} = \frac{3900}{\left(\frac{29.6+24.1}{2}\right) - \left(\frac{23.4+8.2}{2}\right)} = 361\ \left[\frac{W}{K}\right]$$

$$k_{cabin} = \frac{Q_{ACU_{ss}} - Q_{op}}{T_{ambient} - \tilde{T}_{ACU}(t)} = \frac{3600}{(55) - \left(\frac{29.6+24.1}{2}\right)} = 126\ \left[\frac{W}{K}\right]$$

The same method as above can be applied at steady state conditions to find the heat transfer coefficients for the SDU and the TWT-CU. The heat transfer coefficients for the SDU and the TWT-CU are, hence, approximated as follows:

$$k_{hx,SDU} = \frac{Q_{SDU_{ss}}}{\tilde{T}_{SDU} - \tilde{T}_{c,SDU}} = \frac{750}{\left(\frac{22.9+18.5}{2}\right) - \left(\frac{13.4+8.2}{2}\right)} = 76\ \left[\frac{W}{K}\right]$$

$$k_{SDU} = \frac{Q_{SDU_{ss}} - Q_{SDU_{electronics}}}{\tilde{T}_{ACU} - \tilde{T}_{SDU}} = \frac{750-400}{\left(\frac{29.6+24.1}{2}\right) - \left(\frac{22.9+18.5}{2}\right)} = 61\left[\frac{W}{K}\right]$$

$$k_{hx,TWT} = \frac{Q_{TWT,radar}}{\tilde{T}_{PAO} - \tilde{T}_{c,TWT-CU}} = \frac{4000}{\left(\frac{26.3+19.6}{2}\right) - \left(\frac{26.4+8.2}{2}\right)} = 708\ \left[\frac{W}{K}\right]$$

Further, using the similarity of the SDU and the TRU one can assume that the heat transfer coefficients are the same for the two subsystems. This assumption is also necessary to make since the temperature data from [4] of the TRU EGW return is corrupt. The heat transfer coefficients for the TRU are therefore approximated as follows:

$$k_{hx,TRU} = k_{hx,SDU} = 76\ \left[\frac{W}{K}\right]$$

$$k_{TRU} = k_{SDU} = 61\ \left[\frac{W}{K}\right]$$

With the approximated heat transfer coefficients and relationship in Equation (12) it is possible to get an indication of the total heating power at steady state for the TRU according to:

$$Q_{TRU_{ss}} = Q_{TRU,electronics} + k_{TRU}\left(\tilde{T}_{ACU} - \tilde{T}_{TRU}\right)$$
$$= 400 + 61 \cdot \left(\frac{29.6 + 24.1}{2} - \frac{29.5 + 21.3}{2}\right) = 487\ [w]$$

Now, the inequality in Equation (15) can be fully described according to:

$$Q_{total} = 4000 + (3600 + 300) + 487 + 750 \leq 11\,000\ [\text{w}] \quad \textbf{(17)}$$

With the relationships presented in this section it is possible to model the heat transfer that occurs between the different subsystems in ARTHUR.

4.3 Dynamics in LCU, TWT and ACU's Resistance

The EGW is cooled in the LCU and its dynamical behavior is assumed to be equal to a first order system. The time it takes for the EGW to circulate inside the LCU and be cooled is assumed to be approximately five seconds, which gives a time constant $\tau_{LCU} = 5\ s$ [14].

From a log in [4] it is clear that the TWT has a startup time from the instant when the whole ARTHUR system is started until the TWT subsystem actually is able to start. The delay, $\tau_{TWT,delay} = 12\ min$, is implemented in the model to simulate correct startup of the TWT and also to simplify the comparison with the SP data. The dynamical behavior of the TWT can be found in [15], where it is clear that the TWT-power acts as a first order system with a time constant $\tau_{TWT,} \approx 120\ s$.

In Section 3.2 the dynamical behavior of the ACU's resistance has been shown and it has been implemented in the model as a first order system with a time constant $\tau_{Resistance} = 230\ s$.

5 Simulation Results and Comparison with SP Data

This section will present a few different simulation scenarios and compare the simulation results with temperature data from SP (see Section 3.3). Results from simulations with an ambient temperature of 55 ˚C and a thermostat setting of 29 ˚C are presented in this section. The configuration of the AVTA valves can be changed in the simulation and will effectively change the simulation results.

5.1 Default AVTA Configurations

SAAB's default configuration of the valves should, according to Section 3.1.1, give the following control range for the valves:

- TRU valve: 2.0 → 43-63 ˚C
- SDU valve: 1.5 → 33-53 ˚C
- TWT-CU valve: 2.0 → 20-40 ˚C
- ACU valve: 2.7 → 34-54 ˚C

The simulation results that are presented in this section, using the above valve configurations, are shown together with the SP data in sub graphs, respectively. Note that the start time, ~16 min, in the simulation is different from the system's start time, ~48 min, in the SP data.

The comparison of the ACU results, see Figure 5.1, shows the time from system start until the temperature of the ACU has reached the thermostat's temperature setting as follows:

- Simulation ACU: 114 min (130 min)
- SP data ACU: 107 min (155 min)

The simulation results match the SP data rather well. Although the simulation gives a more linear behavior the time constants are in the same region.

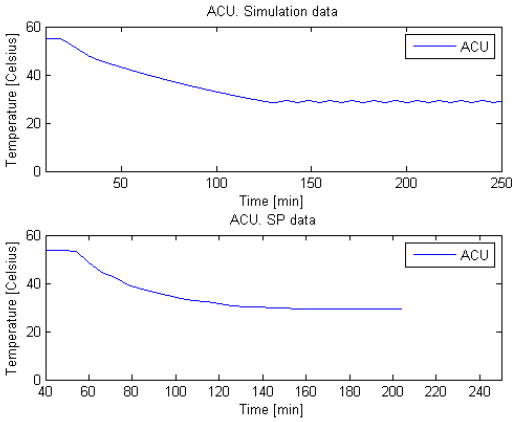

Figure 5.1 Comparison of simulation data and SP data for the ACU.

The comparison of the EGW supply data, see Figure 5.1, clearly shows a difference in time until the desired cold EGW temperature has been reached. The simulated EGW temperature does not reach the LCU set point temperature as fast as it should according to SP data, as follows:

- Simulation EGW supply: 114 min (130 min)
- SP data EGW supply: 52 min (100 min)

In Figure 5.2 one can see an increase of the simulated EGW temperature at $t \approx 30$ min that has quite a big impact on the time it takes to reach the set point temperature. The source of the increase is the startup of the TWT which has been mentioned in Section 4.3.

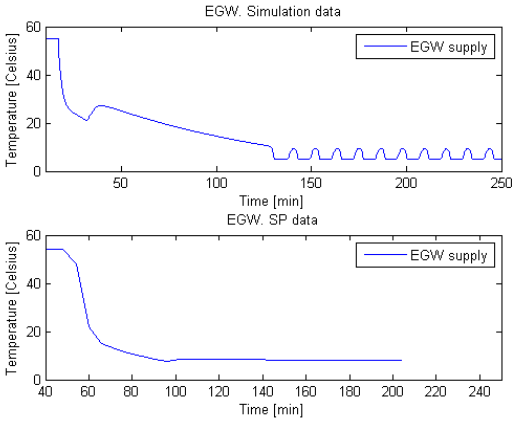

Figure 5.2 Comparison of simulation data and SP data for the EGW supply.

The simulation provides the theoretical EGW flow into the different subsystems and it is clear from Figure 5.3 that the ACU and the TWT-CU needs more EGW flow compared to

the SDU and the TRU. The SDU and the TRU does not need much EGW to be able to cool the electronics, but in contrast, the ACU needs a lot of cooling power to be able to cool the mass of the cabin.

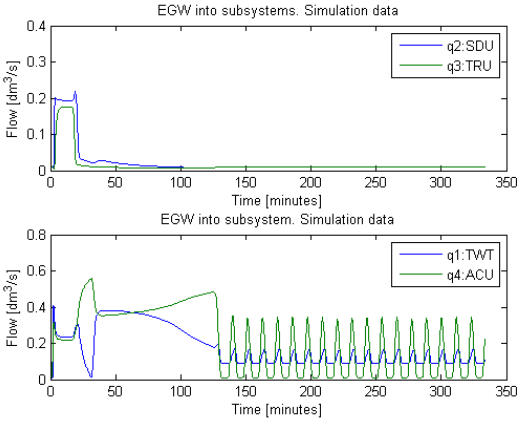

Figure 5.3 Simulation data of the EGW flow.

From the simulation results of the ACU, the EGW supply and the EGW flow, one can note that there are oscillations present in the system. The reason behind the oscillations is the override function in the ACU which creates an ON/OFF behavior of the ACU's resistance and consequently influence the temperature sensor, see Figure 5.4. If the cabin temperature has been decreased to the thermostat setting the ACU's resistance will be switched off, see Figure 5.4 at $t = 125$ min, and consequently the ACU's sensor temperature will cool down from 50 ˚C. When the ACU's sensor temperature approaches the low control area for the ACU's valve, then the cabin temperature will start to increase and the resistance will be switched on again, see Figure 5.4 at $t = 135$ min.

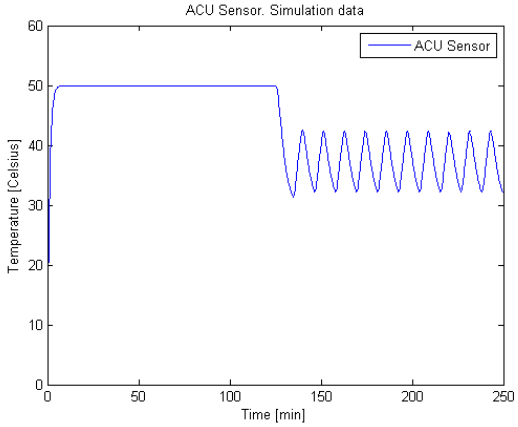

Figure 5.4 Simulation data of the ACU sensor.

The simulation data of the SDU unfortunately does not show the same temperature of the SDU box as the SP data. The simulation is based on a valve configuration that cannot provide such a low temperature, according to Section 3.1, because the valve would be closed at that temperature. Since the ACU temperature affects the temperature of the SDU, it is clear from Figure 5.5 that the time constants are similar to those found for the ACU. The time until the SDU reaches the set point temperature is as follows:

- Simulation SDU: 114 min (130 min)
- SP data SDU: 117 min (165 min)

Given that the SDU and the TRU are similar in regards to its mass and the size of its heat exchanger, it is not surprising that the characteristics of the TRU are very similar to the SDU, see Figure 5.6.

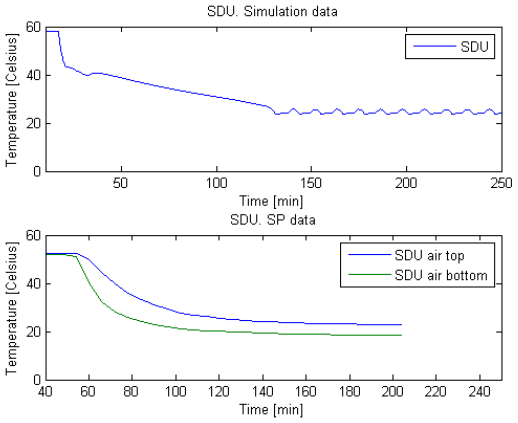

Figure 5.5 Comparison of simulation data and SP data for the SDU.

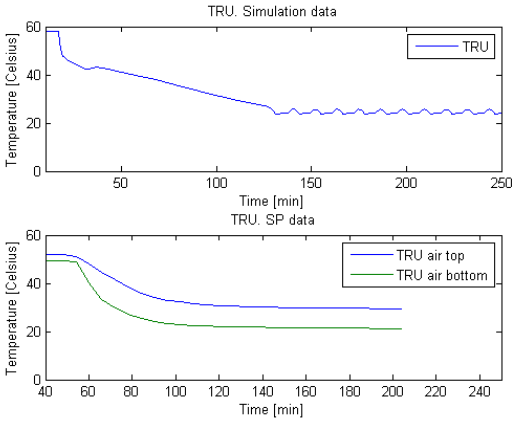

Figure 5.6 Comparison of simulation data and SP data for the TRU.

The simulation data of the EGW temperature out from the SDU does not reach the set point temperature as fast as the SP data, see Figure 5.7. It is a consequence of the earlier mentioned inaccuracy of the EGW supply temperature, which obviously has a large influence on the characteristics of the EGW out from the SDU.

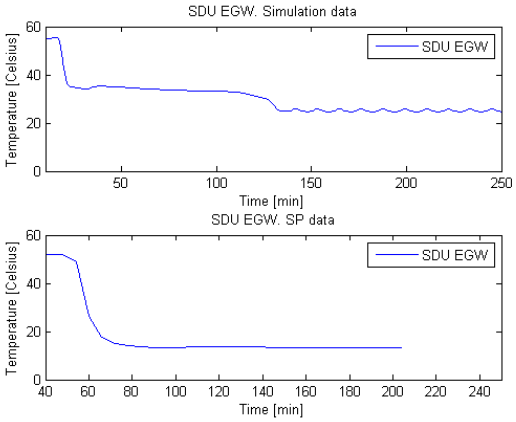

Figure 5.7 Comparison of simulation data and SP data for the EGW temperature out from the SDU.

It is noticeable from the simulation results of the TWT-CU that there is a quick temperature drop of the PAO. This occurs when the TWT has not yet been started, thus the PAO is quickly cooled down. At first it seems like the simulated PAO temperature will decrease as fast as the SP data but it is clear from Figure 5.8 that there is a problem with the model of the TWT-CU and the startup of the TWT. In the SP data of the PAO there is no clear indication that the TWT would start at a later time than the rest of the system, meaning there is a conflict of fact because the modeling is based on a log from [4] where it is stated that the TWT is in fact started at a later instant.

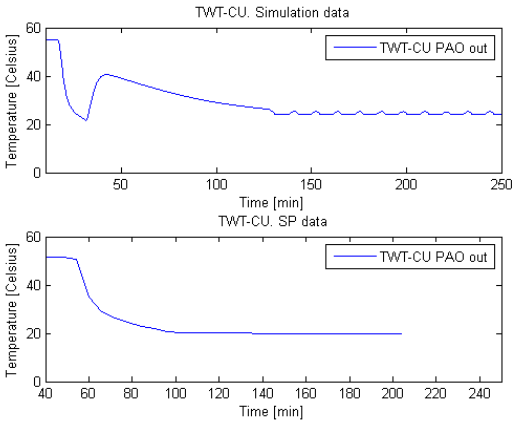

Figure 5.8 Comparison of simulation data and SP data for the PAO temperature out from the TWT.

5.2 Decreased AVTA Configuration for the SDU

A different valve configuration gives an indication of the models response to a changed operating condition. The decreased spring configuration of the SDU valve and default configurations of the other three valves should, according to Section 3.1.1, give the following control range for the valves:

- TRU valve: 2.0 → 43-63 ˚C
- SDU valve: 0.5 → 7-23 ˚C
- TWT-CU valve: 2.0 → 20-40 ˚C
- ACU valve: 2.7 → 34-54 ˚C

The simulation results that are presented in this section, using the above valve configurations, are shown together with the SP data in sub graphs, respectively. Note, as in Section 5.1, that the system's start time is different for the simulation and the SP data, respectively.

From comparison of Figure 5.9 and Figure 5.5 it is clear that a decrease in the valve configuration results in a decreased temperature of the SDU. Other effects of the changed configuration are the slightly increased time constant, but also the more similar characteristics compared to the SP data. The time until the SDU reaches the set point temperature is as follows:

- Simulation SDU: 124 min (140 min)
- SP data SDU: 117 min (165 min)

Further, to achieve a lower temperature the SDU now demands more EGW flow than the TRU which can be seen in Figure 5.10.

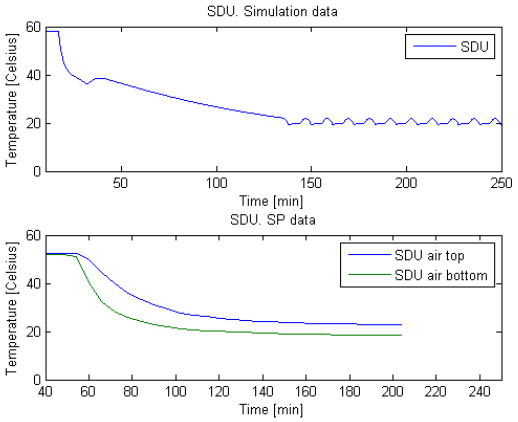

Figure 5.9 Comparison of simulation data and SP data for the SDU, with decreased valve configuration.

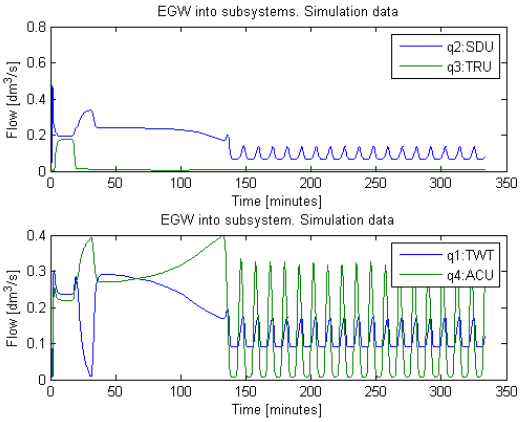

Figure 5.10 Simulation data of the EGW flow, with decreased valve configuration.

Expectedly, the EGW out from the SDU has a more accurate set point temperature, see Figure 5.11, in comparison to the simulation data of Section 5.1. However, the time constant for the EGW is slightly increased in the same way it was for the SDU box.

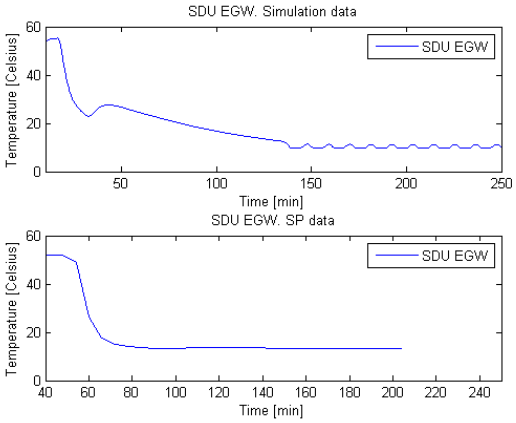

Figure 5.11 Comparison of simulation data and SP data for the EGW temperature out from the SDU, with decreased valve configuration.

5.3 Increased LCU Cooling Power

As mentioned earlier in this report the LCU is known to be somewhat over-sized. Therefore, simulations are run with an increased LCU cooling power to investigate the possibility that the cooling system should be modeled with a larger cooling power. In this section the LCU's

cooling power is increased from 11 kW to 13 kW. However, all other conditions are the same as in Section 5.1, e.g., AVTA configurations, thermostat setting and simulation start time.

The simulated EGW supply for a LCU cooling power of 11 kW and 13 kW are shown in Figure 5.12 and Figure 5.13, respectively. From a comparison of the simulation results it is clear that the EGW supply temperature is decreased much faster with the larger cooling power. Additionally, with the larger cooling power the LCU can achieve the set point temperature of 5 ˚C without the oscillations that originate from the changes in the EGW return temperature.

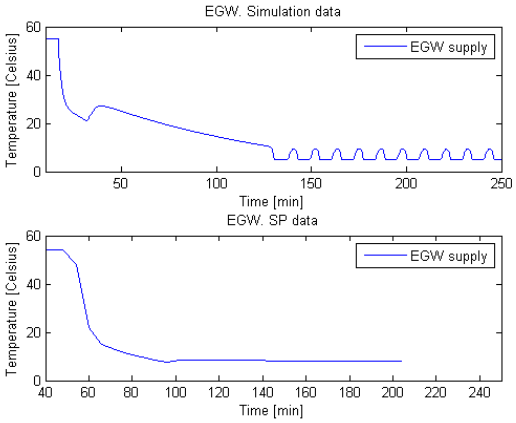

Figure 5.12 Comparison of simulation data and SP data for the EGW supply, with 11 kW.

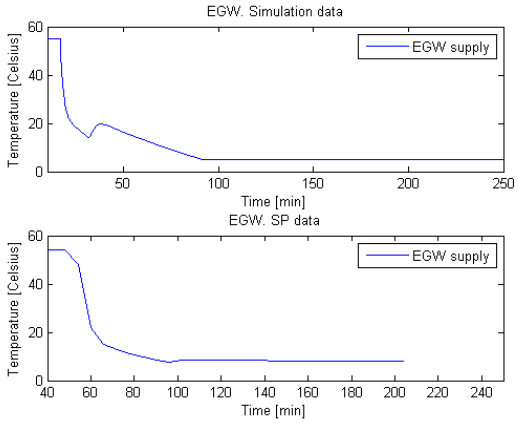

Figure 5.13 Comparison of simulation data and SP data for the EGW supply, with 13 kW.

The EGW temperature does not reach the LCU set point temperature as fast as it should according to SP data, but it is much closer compared to the results from Section 5.1:

- Simulation EGW 13 kW: 69 min (85 min)
- SP data EGW: 52 min (100 min)
- Simulation EGW 11 kW: 114 min (130 min)

A faster cooling of the EGW supply obviously has consequences to the rest of the cooling system. From Figure 5.14 and Figure 5.15 it is clear that the temperature of the ACU and the TRU reaches the set point temperatures faster than in the simulation results in Section 5.1. In fact, the time from system start until the set point has been reached is shorter than in the SP data.

- Simulation ACU 13 kW: 79 min (95 min)
- SP data ACU: 107 min (155 min)
- Simulation TRU 13 kW: 79 min (95 min)
- SP data TRU: 92 min (140 min)

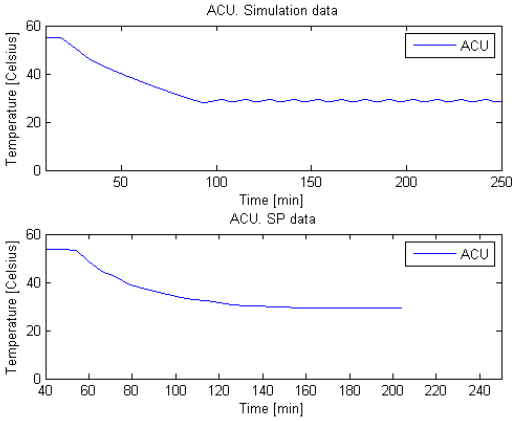

Figure 5.14 Comparison of simulation data and SP data for the ACU, where cooling power is 13 kW.

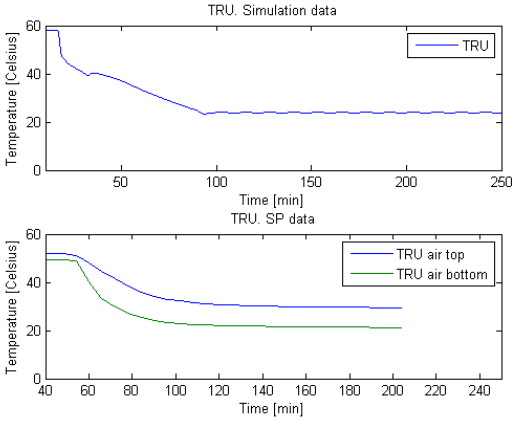

Figure 5.15 Comparison of simulation data and SP data for the TRU, where cooling power is 13 kW.

Further, the characteristics of the simulation data and the SP data are more similar to each other with the increased cooling power. The removal of most of the oscillations in the EGW supply results in smaller oscillations, in for example the ACU and the TRU, than in the simulation data for the 11 kW cooling power. In Figure 5.15, it is noticeable that the effect of the TWT startup on the TRU temperature is not significant anymore. At the startup of the TWT, the large cooling power is enough to start cooling the TWT and also continue to cool the TRU.

6 Discussion

This section will first present a discussion on the performance of the control that is used today in ARTHUR. Secondly, an evaluation of the model's validity and a discussion about the simplifications made in the model will be presented. Finally, the third subsection is based on a discussion with several SAAB employees regarding possible improvements to the control system.

6.1 Evaluation of Present Control

The AVTA valves that are used in the cooling system for ARTHUR are simple to setup and have a large temperature operating range. They have been used in ARTHUR for a long time and their performance so far has been of good enough standard. However, there has been uncertainty as to how the AVTA valves function. This has raised questions during tuning attempts of the cooling system. In this report, the temperature characteristics of the AVTA valves have been defined which gives a better understanding of the valves, their control range and their functionality. It can be concluded that the valves have a maximum opening area and an increase in temperature will not open the valves further. Additionally, the maximum opening area has been found to be equal for differently configured springs. The control of the cooling system is still limited by a few drawbacks of the AVTA valves but the findings of this report assist in tuning the spring configuration of the valves, e.g., tuning the configuration of the ACU valve. To make sure that the ACU valve is fully open when the ACU resistance is ON, it is necessary to at least decrease the spring configuration from 2.7 to 2.5.

Repeatability of the AVTA valves has not been presented in this report but it has been noted throughout this project that there is a problem with the valve's springs. On several occasions experiments had to be repeated because the valve opening size did not change with an increase of temperature. For an unknown reason the spring would lock in a certain position and one had to adjust the spring configuration to get the valve to start regulating correctly again.

The fact that the AVTA valves are analogue simplifies the setup and suggests the property of robustness against electrical errors but it also means that the valves are limited in their control performance. This limitation, together with the placement of the AVTA valves in

unreachable locations, results in a disadvantage in regards to flexibility of the control. A clear example was the problem with the ACU valve where the operators should be able to manually change the temperature inside the cabin, but they could not because the spring could not be re-configured during operation. Therefore a type of override function had to be created for the ACU, which itself causes bad comfort for the operators because of its ON/OFF behavior.

6.2 Evaluation of Model

ARTHUR's climate system is large and complex and the model presented in this report is a simplified version of that system. The presented simulations have been run with configurations which makes it possible to compare and evaluate the results with data from SP. However, it is possible to simulate different thermostat and spring configurations but then there is no available data to compare with. Simulation results cannot be fully evaluated and therefore it is only possible to use the model as an indication of the climate system's behavior at different conditions.

The modeling process included several simplifications and assumptions, e.g. the cabin temperature was modeled uniformly, the air flow was not considered, and the heat transfer coefficients were approximated, which means that there are several sources of error in the model. Considering that it is a simplified model one should not draw too large conclusions from the simulation results. Although, it is possible to use the results to get a better overview of the cooling system, e.g., notice the dynamic distribution of the EGW flow. Further, the subsystems' time constants from the simulation are not that different from the time constants of the SP data and consequently the model can provide a reasonable indication of the time it takes to reach the set point temperatures.

The experiments on the AVTA valves, especially regarding the dynamic behavior of the valves, were more time consuming than expected and caused delays in this project. It can be concluded from the results of the temperature experiments that the time constants of the valves are very small in comparison to the time constant of the cabin. In view of the results of the valve's dynamical properties, perhaps a better focus of the modeling process would have been to investigate the heat exchangers in more depth. A better background for approximating the heat transfer coefficients would have given more trust in the simulated heat exchange and consequently increased the accuracy of the model. Nonetheless, it was valuable to investigate the valves thoroughly to be able to reduce the uncertainty of their characteristics and dynamics.

The simulation results do not show a low set point temperature of the EGW supply as fast as the SP data, which means an uncertainty in the model's ability. As mentioned in this report, it is known that the LCU cooling power is over-dimensioned and therefore more cooling power is added to the LCU to see if this could improve the accuracy of the model. With the increased cooling power, one can notice a faster temperature drop of the EGW supply which could mean that the LCU in fact has a cooling power larger than 11 kW.

As mentioned, it is necessary to increase the accuracy of the model to be able to draw further conclusions from the simulation results. However, if improvements are made to the model, then there is potential to implement alternative control schemes in Simulink and compare the simulation results. Unfortunately, this report will only discuss and suggest possible alternatives for control hence, no product search has been performed.

6.3 Suggestion of New Control

The valves used today at SAAB EDS get the job done in a fairly good manner. However, as pointed out in this report, the valves have drawbacks and a better performing control of the cooling system would be desirable. A modern alternative for new control would be to implement a PLC together with several new sensors and new valves, which could monitor and control the EGW flow into each subsystem.

There is not much space available for the present AVTA valves because there are high demands to keep the size of each subsystem's box at a minimum. A new type of valve would have to be of similar dimensions to fit inside the subsystem's box. It would be possible to use a magnetic valve but it is not preferable because of the lack of functionality to continuously regulate the opening size, and further the valve's likely introduction of oscillatory behavior to the system. As a replacement, motor controlled valves would be beneficial because of their continuous regulating capabilities and their precision. However, a potential problem with motor controlled valves is their tendency to have large dimensions. The challenge with finding a suitable motor controlled valve is finding a product that has a small size and also has the possibility to operate in a large temperature range.

To enable the possibility to implement a larger valve it might be necessary to change the placement of the valves. Instead of placing the valves inside the respective subsystem's box they could be placed closer to the LCU, e.g., where the EGW flow is divided into each subsystem's pipe.

If new sensors, e.g., temperature sensors and flow meters, are placed at appropriate locations, a PLC would have enough information to be able to regulate the motor controlled valves and consequently control the whole cooling system. The intelligence of the control system would increase and in comparison to the present control a PLC would be able to perform the control in a more flexible way, e.g., the ACU's override function could be removed and the subsystems could have different set points depending on the ambient temperature. During warm ambient temperatures, a PLC could execute a low set point temperature for the SDU and the TRU so that the radar system can start quickly. When the radar system has been started, a PLC could execute a new higher set point temperature for the SDU and the TRU to counteract the problem with condensation inside the two subsystem's boxes. Consequently, this would result in slow cooling of the cabin air and discomfort for the operators but faster startup of the radar system.

References

[1] R. Johansson and M. Villiamsson, Control of Liquid Cooling Unit, MSc thesis, Report No. EX029/2010: Chalmers University of Technology, 2010.

[2] R. Shah and D. Sekulic, Fundamentals of Heat Exchanger Design, John Wiley and Sons, United States of America, ISBN 0-471-32171-0, 2003.

[3] T. Glad and L. Ljung, Reglerteknik - Grundläggande teori, Studentlitteratur, ISBN 9789144022758, 2006.

[4] Internal SAAB EDS report, "Verification Record for ARTHUR WLS," 2011.

[5] Internal SAAB EDS report, "Product Specificaion Liquid Cooling Unit," 2009.

[6] Internal SAAB Wiki, "ARTHUR," [Online]. Available: https://pd.gg.smw.saab.se/index.php5/ARTHUR. [Accessed 2011-12-20].

[7] Internal SAAB EDS report, "Konstruktionsspecifikation ARTHUR ITALIEN Klimatsystem," 2010.

[8] Anderol, "Anderol Product Data Sheet," [Online]. Available: http://www.qclubricants.com/msds/PDS/Royco602.pdf. [Accessed 2011-12-20].

[9] Internal SAAB EDS report, Product Specification Magnetic Drive Gear Pump and Motor, 2008.

[10] Danfoss, "Thermostatic Valve – AVTA," [Online]. Available: http://www.ra.danfoss.com/TechnicalInfo/Literature/Manuals/04/ICPD500A302.pdf. [Accessed 2011-12-20].

[11] Danfoss, "AVTA, Thermostatic valves with temperature sensitive sensor," [Online]. Available: http://www.danfoss.com/Products/Categories/Faqs/IA/Thermostatic-valves/AVTA-Thermostatic-valves-with-temperature-sensitive-sensor/a77737a3-66b7-469b-9a2c-bc028e5e92b5.html. [Accessed 2011-12-20].

[12] Grundfos, "Kv-värde," [Online]. Available: http://cbs.grundfos.com/GSV_Sweden/lexica/HEA_kv_value.html#-. [Accessed 2011-12-20].

[13] I. Granet and M. Bluestein, Thermodynamics and Heat Power, Prentice Hall, United States of America, 6th edition, ISBN 0-13-021539-2, 2000.

[14] P. Bung, Interviewee, *LCU Performance*. [Interview]. 2011.

[15] Internal SAAB EDS report, "ArthurItSöndag," 2011.